Environmental Science Processes & Impacts

ROYAL SOCIETY OF CHEMISTRY

PAPER

View Article Online
View Journal | View Issue

Check for updates

Cite this: *Environ. Sci.: Processes Impacts*, 2025, **27**, 3482

Critical biotransformation half-lives of chemicals in air-breathing wildlife to assess food-chain bioaccumulation and biomagnification

Roman Ashauer *[ab]

Biomagnification, the process by which chemical concentrations increase in organisms at higher trophic levels, can pose significant risks to wildlife and ecosystems. Despite its importance, our understanding of species-specific differences in biomagnification potential remains limited. The analysis of the critical biotransformation half-life, the maximum half-life to avoid biomagnification of a chemical, can help address this gap. Here, I present a comprehensive analysis of critical biotransformation half-lives across diverse air-breathing wildlife species, providing novel insights into the factors influencing biomagnification. By constructing species-specific contour plots in chemical partition space, I reveal substantial variations in biomagnification potential among different organisms, with differences in critical biotransformation half-lives reaching more than two orders of magnitude. These substantial interspecies differences underscore the need for species-specific biotransformation data and biomagnification modelling. This analysis also demonstrates that model normalisation methods significantly impact these species-specific differences, suggesting that the choice of normalisation can alter biomagnification assessments. I further delineate the chemical partition space regions where elimination is dominated by urination *versus* respiration, highlighting important interspecies variations. Finally, I introduce a weight-of-evidence approach for assessing potential food-chain biomagnification, illustrated through a case study on methoxychlor, which is a generalizable approach that differs from current approaches by its stronger focus on biotransformation. A critical discussion of allometric scaling and sources of uncertainty identifies further research needs. This work enhances our ability to predict and assess biomagnification risks across diverse ecosystems and species, offering valuable tools for environmental risk assessment and conservation efforts.

Received 21st March 2025
Accepted 11th September 2025

DOI: 10.1039/d5em00220f

rsc.li/espi

Open Access Article. Published on 18 irailak 2025. Downloaded on 2026/04/18 18:27:39.
This article is licensed under a Creative Commons Attribution 3.0 Unported Licence.

Environmental significance

Biomagnification of chemicals in food chains can pose a significant risk to wildlife and ecosystems. This study addresses a critical knowledge gap in species-specific differences in biomagnification potential. By analyzing critical biotransformation half-lives across diverse air-breathing wildlife across chemical partition space, I reveal substantial variations in biomagnification potential among organisms and the dependence of those interspecies differences on chemical partitioning. This work enhances our ability to predict and assess biomagnification risks across diverse ecosystems and species. By introducing a weight-of-evidence approach for assessing potential food-chain biomagnification, illustrated through a case study, I provide a generalizable approach that differs to current approaches by its stronger focus on biotransformation.

Introduction

Synthetic chemicals can bioaccumulate and some biomagnify along food-chains[1–3] and this can pose a risk to humans and wildlife. Biomagnification means that concentrations in biological organisms increase with trophic level.[4] More accurately biomagnification is characterized by an increase in fugacity in the organism over its food and is explained by digestion of lipids in the gastrointestinal tract, leading to solvent depletion and solvent switching.[5–7] Whether biomagnification occurs depends on the physical and chemical properties of the substance as well as biological traits of the species comprising the relevant food-chains. Biomagnification can be quantified with a biomagnification factor (BMF), defined as the ratio of the fugacity in the organism and the fugacity in its diet at steady-state, and when the BMF is greater than one, biomagnification occurs. Instead of using fugacities, the BMF can also be calculated as the ratio of appropriately normalized concentrations in the organism and its diet.[4] Because biomagnification is defined operationally for the purpose of assessing potential chemical risks and informing regulatory decisions, it is generally assessed by comparing concentrations of a chemical in organisms at different trophic levels (*i.e.*, in predators relative to their prey). For that purpose, it is desirable to reduce variability in the calculation of the BMF caused by differences in body composition of organisms

[a]*Department of Environment and Geography, University of York, York YO10 5NG, UK*
[b]*Syngenta Crop Protection AG, Rosentalstr. 67, 4058 Basel, Switzerland. E-mail: roman.ashauer@syngenta.com*

This journal is © The Royal Society of Chemistry 2025

Open Access Article. Published on 18 irailak 2025. Downloaded on 2026/04/18 18:27:39. This article is licensed under a Creative Commons Attribution 3.0 Unported Licence.

through normalization,[4] specifically differences in the amount and composition of sorptive phases in the organism and its diet. Lipid-normalization which accounts for different lipid contents and lipid-equivalent normalization, which accounts for differences in body lipid, protein, carbohydrate and water content, are two normalization methods,[4,8–11] whilst the fugacity approach is another.[3,12]

There are many well established regulatory frameworks to assess biomagnification and bioaccumulation in water-breathing (aquatic) organisms and more recently the assessment of air-breathing (terrestrial) species is receiving increased attention too.[13,14] Some models for bioaccumulation and biomagnification in air-breathing species and terrestrial food-chains are already available[1,2,9,15,16] and some are even integrated into user-friendly assessment tools.[17] Assessing the potential of chemicals to biomagnify in air-breathing species requires considering their partitioning between body and air and body and water, as well as understanding the chemical's biotransformation in the relevant species. Biotransformation, sometimes also termed metabolic transformation (metabolism), is the biochemical break-down of the parent chemical into transformation products, which are usually less toxic, more water soluble and thus easier to transport out of the body.

Generally, we do not know the biotransformation pathways and rate constants of chemicals in wildlife (see *e.g.*[18] for birds). Yet, the biotransformation half-life, which can be calculated from the biotransformation rate constant, is a key parameter in models to calculate BMFs. This poses a challenge for assessing the biomagnification potential of chemicals, especially in wildlife, because this assessment relies strongly on modelling that requires the generally unknown biotransformation half-life as input. Consequently, we still have very limited knowledge of actual bioaccumulation and biomagnification of chemicals in wildlife.

To work around the problem of unknown biotransformation, one can plot biotransformation half-life values as functions of partition ratios, as demonstrated using models parameterized for humans by Goss *et al.*[19] and Arnot *et al.*.[20] Gobas *et al.* have suggested using biotransformation half-life values to assess the potential of a substance to biomagnify in terrestrial organisms more generally.[21] Recently, Saunders & Wania[9] published a model to calculate the lipid-equivalent normalized BMF for neutral organic substances at steady-state for a wide range of air-breathing wildlife and, importantly, Saunders & Wania also published a very comprehensive set of species-specific model parameters. Thus, we know the importance of biotransformation for biomagnification, the use of partition space plots to illustrate patterns across chemical space and we have BMF models for a wide range of air-breathing species. What we poorly understand is the interplay between biotransformation, a chemical's partition properties and biological differences amongst species in biomagnification modelling.

Improving this understanding is the aim of this study. To do so, I calculate and plot the critical biotransformation half-life in a diverse range of air-breathing wildlife and construct species-specific contour plots of that parameter in chemical partition space. The critical biotransformation half-life is the maximum half-life to avoid biomagnification of a chemical. Shorter biotransformation half-lives do not result in biomagnification. Biotransformation half-lives longer than the critical half-life value do result in biomagnification. The critical biotransformation half-life is specific for the respective combination of $\log K_{OA}$ (octanol-air partition ratio) and $\log K_{OW}$ (octanol-water partition ratio) of the chemical and it is specific for each biological species. I also investigate how model versions with different normalisation methods result in species-specific differences in critical half-lives and I calculate for which part of the chemical partition space elimination is dominated by urination *vs.* respiration and how that differs across species. Finally, I illustrate a weight of evidence approach to assess potential food-chain biomagnification.

Materials & methods

Model 1: kinetic biomagnification model (not normalised).

A simple biomagnification model that assumes dietary uptake dominates is given by:

$$\mathrm{BMF_k} = \frac{E_D G_D}{k_T} \quad (1)$$

where subscript D refers to Diet, E_D is the dietary uptake efficiency [unitless] (the fraction of chemical absorbed into the body from the ingested food), G_D is the weight normalized feeding rate [$\mathrm{kg_{diet}\ kg_{organism}^{-1}\ d^{-1}}$], k_T is the total elimination rate [$\mathrm{d^{-1}}$] and $\mathrm{BMF_k}$ is the kinetic biomagnification factor [$\mathrm{kg_{diet}\ kg_{organism}^{-1}}$]. This model does not include fugacity-, lipid- or lipid-equivalent normalisation; however, it is the model one would use to calculate the ratio of actual (not normalized) concentrations in the organism and its diet at steady-state. It is a simplified model where uptake is only *via* the diet and other routes (*e.g.* inhalation, drinking, skin) are not considered.

Saunders & Wania[9] included only urinary excretion and respiratory exhalation as elimination pathways, omitting biotransformation (implicitly assuming no biotransformation occurs) because the biotransformation rate is generally unknown, to model elimination as:

$$k_T = k_U + k_R = \frac{G_{urination}}{v_{vol_oct_eq_organism} \times K_{OW}(T_B)} + \frac{G_{respiration}}{v_{vol_oct_eq_organism} \times K_{OA}(T_B)} \quad (2)$$

where subscript B refers to Biota, k_R is the rate constant for excretion *via* respiration [$\mathrm{d^{-1}}$] and k_U is the rate constant for excretion *via* urination [$\mathrm{d^{-1}}$], $G_{urination}$ is the weight normalized urination rate at body temperature [$\mathrm{L_{urine}\ d^{-1}\ kg_{organism}^{-1}}$], $G_{respiration}$ is the weight normalized animal respiration rate [$\mathrm{L_{air}\ d^{-1}\ kg_{organism}^{-1}}$], $v_{vol_oct_eq_organism}$ is the volume of octanol equivalent in the body [$\mathrm{L_{octanol}\ kg_{organism}^{-1}}$], K_{OA} is the octanol-air partition ratio [$\mathrm{L_{air}\ L_{octanol}^{-1}}$], K_{OW} is the octanol-water partition ratio [$\mathrm{L_{water}\ L_{octanol}^{-1}}$] and T_B is the body temperature [°C]. Here, I use the model of Saunders & Wania for the urinary excretion and respiratory exhalation pathways, and, in addition, I model biotransformation with a single-first order kinetics loss term:

$$k_T = \frac{G_{urination}}{v_{vol_oct_eq_organism} \times K_{OW}(T_B)} + \frac{G_{respiration}}{v_{vol_oct_eq_organism} \times K_{OA}(T_B)} + \frac{\ln 2}{HL} \quad (3)$$

Open Access Article. Published on 18 irailak 2025. Downloaded on 2026/04/18 18:27:39. This article is licensed under a Creative Commons Attribution 3.0 Unported Licence.

where HL [d] is the whole-body biotransformation half-life. *i.e.* the whole-body biotransformation half-life that results in a BMF equal to one. Shorter half-lives, indicating faster biotransformation, lead to BMF values below one and therefore no biomagnification occurs for such substances in the species modelled (see also[19,21]). Setting BMF_k equal to one, such that $k_T = E_D \times G_D$, yields eqn (4), where the critical biotransformation half-life $HL_{crit.biotransf.}$ [d] is:

$$HL_{crit.biotransf.} = \ln 2 \Big/ \left(E_D \times G_D - \frac{G_{urination}}{v_{vol_oct_eq_organism} \times K_{OW}(T_B)} - \frac{G_{respiration}}{v_{vol_oct_eq_organism} \times K_{OA}(T_B)} \right) \quad (4)$$

Model 2: model for hydrophobic chemicals (model normalised, high K_{OW})

The first model (their eqn (1)) used by Saunders & Wania[9] to calculate the lipid-equivalent normalised BMF[8] for neutral organic substances at steady-state is given by:

$$BMF_L = \frac{E_D G_D}{k_T} \times \text{normalisation} \quad (5)$$

where BMF_L is the lipid-normalized biomagnification factor [kg_{lipid} kg_{lipid}^{-1}] and normalisation is a term that differs depending on the applicability domain of the model. For hydrophobic chemicals that accumulate predominantly in neutral lipids, the normalisation term is the ratio of the fractional lipid equivalent content of diet [kg_{lipid} kg_{diet}^{-1}] divided by the fractional lipid equivalent content of body [kg_{lipid} $kg_{organism}^{-1}$].[9,21] Thus, this is the equation to calculate the lipid-equivalent normalized, whole-body, critical biotransformation half-life $HL_{crit.biotransf.}$ [d] for hydrophobic neutral organic substances:

$$HL_{crit.biotransf.} = \ln 2 \Big/ \left(E_D \times G_D \times \frac{f_{lipid_eq_diet}}{f_{lipid_eq_organism}} - \frac{G_{urination}}{v_{vol_oct_eq_organism} \times K_{OW}(T_B)} - \frac{G_{respiration}}{v_{vol_oct_eq_organism} \times K_{OA}(T_B)} \right) \quad (6)$$

where $f_{lipid_eq_diet}$ is the fractional lipid equivalent content of diet [kg_{lipid} kg_{diet}^{-1}], $f_{lipid_eq_organism}$ is the fractional lipid equivalent content of body [kg_{lipid} $kg_{organism}^{-1}$].

Model 3: model for hydrophobic and hydrophilic chemicals (model normalised, all K_{OW})

A BMF model that is applicable also for hydrophilic chemicals requires a more complex normalisation term and was defined in eqn (14) in Saunders & Wania.[9] This model is applicable for substances across the whole range of K_{OW} values, because it also accounts for partitioning into body water. Partitioning into body water is important when comparing different species because species differ in their water content. Based on this more widely applicable model the equation to calculate the whole-body, critical biotransformation half-life $HL_{crit.biotransf.}$ [d] is:

$$HL_{crit.biotransf.} = \ln 2 \Big/ \left(E_D \times G_D \times \text{normalisation} - \frac{G_{urination}}{v_{vol_oct_eq_organism} \times K_{OW}(T_B)} - \frac{G_{respiration}}{v_{vol_oct_eq_organism} \times K_{OA}(T_B)} \right) \quad (7)$$

with

$$\text{Normalisation} = \frac{\Phi_{L,D} + \Phi_{P,D}\beta + \Phi_{C,D}\theta + \Phi_{W,D}/K_{ow}}{\Phi_{L,B} + \Phi_{P,B}\beta + \Phi_{C,B}\theta + \Phi_{W,B}/K_{ow}} \quad (8)$$

where and Φ_L is the fraction lipid [kg_{lipid} $kg_{biomass}^{-1}$], Φ_P is the mass fraction protein [$kg_{protein}$ $kg_{biomass}^{-1}$], Φ_C is the mass fraction carbohydrate [$kg_{carbohydrate}$ $kg_{biomass}^{-1}$], Φ_W is the mass fraction water [kg_{water} $kg_{biomass}^{-1}$], β is the sorptive capacity of protein relative to lipid (0.05 kg_{lipid} $kg_{protein}^{-1}$)[10] and θ is the sorptive capacity of carbohydrates relative to lipid (0.1 kg_{lipid} $kg_{carbohydrates}^{-1}$).[1]

Further model assumptions and temperature correction

Following Saunders & Wania I also assume equivalent sorptive properties of lipid and octanol, negligible temperature dependence of K_{OW} (*i.e.* $K_{OW}(T_B) = K_{OW}(25\ °C)$)[22] and apply a temperature correction to K_{OA} according to Baskaran *et al.*:[23]

$$\Delta U_{OA} = -8.75 \times \log K_{OA} - 5.07 \quad (9)$$

$$\text{corr_log } K_{OA} = \frac{-\Delta U_{OA}}{R} \times \left(\frac{1}{273.15 + T_B} - \frac{1}{273.15 + 25} \right) \times \log_{10}(e) + \log K_{OA} \quad (10)$$

$$K_{OA}(T_B) = \text{corr_log } K_{OA} \quad (11)$$

where ΔU_{OA} is the internal energy of phase transfer from octanol to air [kJ mol^{-1}], R is the ideal gas constant (8.314×10^{-3} kJ K^{-1} mol^{-1}) and corr_log K_{OA} is the temperature corrected octanol-air partition ratio [L_{air} $L_{octanol}^{-1}$].

Input data

Input data for the model originates from Table S5 of the SI provided by Saunders & Wania[9] and includes 203 datasets. These 203 datasets comprise 141 unique species, of which 34 species have multiple entries. The multiple entries represent different conditions (*e.g.* flight *vs.* resting) and consist of different parameter values for the same species. I have revised the naming of some species with multiple entries in the first column of the file to follow a harmonized naming convention (*e.g.* correcting some typos and misspellings). The revised data file is provided in the SI of this study.

In this dataset only the animal respiration rates are derived directly from species-specific observations. The urination rates were derived by allometric scaling for mammals and birds, and the urination rates for reptiles were derived by adjusting the allometric relationship for birds to the lower body weight of reptiles.[9] The animal feeding rates were calculated from field metabolic rates and energy content of the food, where the field metabolic rates were obtained from allometric relationships for birds, mammals and reptiles.[9] A correction for different body temperatures was applied to the field metabolic rates using a Q_{10} value of 2.5 and the same Q_{10} correction was also applied to urination rates (less ingestion, metabolic activity and urination at lower body temperatures).[9]

Open Access Article. Published on 18 irailak 2025. Downloaded on 2026/04/18 18:27:39. This article is licensed under a Creative Commons Attribution 3.0 Unported Licence.

Data analysis and visualization

I plotted critical half-life values as function of the chemical partition space and created contour plots by calculating a matrix of critical half-life values corresponding to a range of $\log K_{OA}$ values from 0 to 15 and $\log K_{OW}$ values from −2 to 8 with 0.1 spacing (*i.e.* a matrix of 151 $\log K_{OA}$ values and 101 $\log K_{OW}$ values). I calculated this matrix of critical half-life values for each entry (species) in the input data file, saved it as text file and subsequently plotted it (Fig. 1) using the Python contour plotting functionality (see code in SI). Model 1 is eqn (4), model 2 is eqn (6) and model 3 is eqn (7) and (8). The temperature correction (eqn (9)–(11)) is used in all three models.

Next, I compared all the datasets (all species) generated with model 3 with each other and counted chemicals (*i.e.* combinations of $\log K_{OW}$ and $\log K_{OA}$) for which the critical half-life differed by more than 10 days or more than 100 days. I also plotted these frequencies in partition space (Fig. 2).

To better understand for which chemicals elimination, excluding biotransformation, is dominated by each animal's capacity to eliminate the chemical *via* respiration (k_R) or urination (k_U) I calculated and plotted the ratio of both rate constants in a similar matrix corresponding to a range of $\log K_{OA}$ values from 0 to 15 and $\log K_{OW}$ values from −2 to 8 (Fig. 3). The slope of the line that divides the partition space into areas where elimination *via* urination dominates (above the line) *vs.* areas where elimination *via* respiration dominates (below the line) is also calculated.

As an illustrative example I calculated the critical half-lives for methoxychlor (CAS 72-43-5) with model 3 and plotted them against body weight, whilst using different symbols to differentiate different animal categories as well as indicating whether elimination is dominated by urination or respiration (Fig. 4). Table 1 summarises this analysis. I also analysed the correlation in this dataset (Spearman rank correlation coefficient on log transformed data, full analysis in the SI).

Table 1 also includes critical biotransformation half-live values scaled to a standardised weight (1 kg) and temperature (25 °C). These calculations followed the approach described on page 22 of the BAT user manual[24] and involve conversion of half-lives to first-order rate constants in a first step, which are then scaled as:

$$k_{B,s} = k_{B,a}(W_s/W_a)^{-0.25} e^{0.01(T_s - T_B)} \quad (12)$$

Where $k_{B,s}$ is the scaled critical biotransformation rate constant [1/d], $k_{B,a}$ is the actual critical biotransformation rate constant [1/d] before scaling (calculated from the critical biotransformation half-life as $k_{B,a} = \ln(2)/HL_{crit.biotransf.}$), W_s is the weight selected for scaling (here 1 kg), W_a is the actual body weight of the animal [kg], T_s is the body temperature [°C] selected for scaling (here 25 °C) and T_B is the actual body temperature of the animal [°C].

To better understand the differences between the three models I calculated the differences in critical biotransformation half-lives between the three models. Then I selected the combination of $\log K_{OW}$ and $\log K_{OA}$ where the largest difference between any of the three models occurs for a given species and plotted the critical half-life values for the three models (Fig. 5).

Model implementation

I implemented the models in Python and provide the model code, including code for data analysis and visualization, as SI.

Sources of methoxychlor case-study data

I used methoxychlor (CAS 72-43-5) as example chemical because I could easily find the required data and because it has partitioning properties suitable for illustrating biomagnification modelling questions. Using the kinetic model (eqn (4), model (1) I calculated the critical biotransformation half-lives for methoxychlor and the two species of concern in a simple two-species food-chain (Tundra-vole, Red-tailed hawk, see Results & discussion section). I retrieved values for methoxychlor of $\log K_{OW}$ (5.08) and $\log K_{OA}$ (10.244) at 25 °C from the EAS-E suite online tool.[25]

A whole-organism biotransformation rate constant, easily converted to a half-life, was derived by Lee *et al.*[26] for methoxychlor in the rat from *in vitro* experiments (0.252 ± 0.00478 SE h^{-1}). Measured loss of parent after two hours *in vitro* with liver-slices and ^{14}C-labelled methoxychlor yielded half-life data for rat, mouse, quail and trout.[27] Quantitative structure activity relationships (qsar) built into the EAS-E web tool[25] provide estimates of whole-body biotransformation half-lives in human and fish.

Results & discussion

Critical biotransformation half-lives: differences between species

I created contour plots of critical biotransformation half-lives in chemical partition space (K_{OW} *vs.* K_{OA}) for all 203 datasets and using all three BMF models. All contour plots are provided in the SI and Fig. 1 shows the plots for three species (a mammal, reptile and bird) that nicely serve to illustrate the typical differences in the contour plots: diamondback water snake, humming bird (flight) and thirteen-lined ground squirrel. The critical biotransformation half-life depends on the chemical partition space and this chemical partition space plot of the $HL_{crit\cdot biotransf.}$ differs from one species to another (Fig. 1, all Fig. in SI folder "SI HL contour plots"). It is also evident that the required half-life to avoid biomagnification can differ by orders of magnitude for the same chemical in different species (*e.g.* compare Fig. 1d–f *vs.* 1a–c and 1g–i, *i.e.* Hummingbird *vs.* Diamondback water snake and Thirteen-lined ground squirrel).

There are regions in the chemical partition space where large differences in the critical biotransformation half-lives between species are most frequent. When comparing all species with each other (20 503 comparisons), using model 3, I found that differences in critical biotransformation half-lives greater than 10 days (Fig. 2a) or greater than 100 days (Fig. 2b) occur mostly in two areas of partition space. These are the yellow shaded regions in Fig. 2. First, for chemicals with $\log K_{OW}$ approximately between 1 and 3 in combination with a $\log K_{OA}$ greater

Open Access Article. Published on 18 irailak 2025. Downloaded on 2026/04/18 18:27:39.
This article is licensed under a Creative Commons Attribution 3.0 Unported Licence.

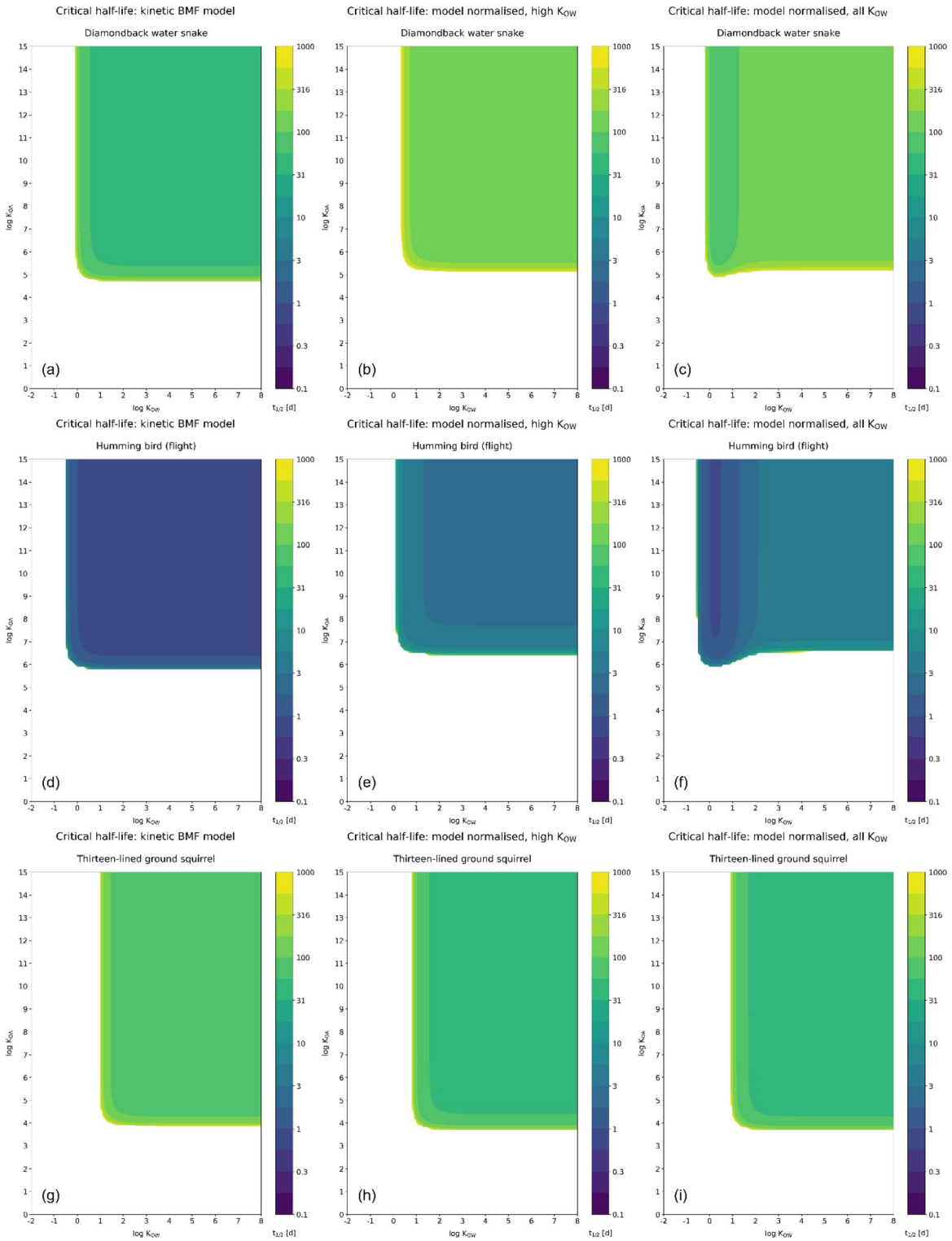

Fig. 1 Contour plots of critical biotransformation half-life values ($t_{1/2}$ [d]) within chemical partition space for three models and three illustrative species (Figures for 3 models and 203 datasets are provided in the SI folder "SI HL contour plots"). Results for the kinetic BMF model (no normalisation, model 1) in the left-hand column, the lipid-normalised BMF (model 2) in the middle and the model normalized for lipid- and water-partitioning (model 3) in the right-hand column. Colours indicate critical biotransformation half-life values, *i.e.* the maximum half-life to avoid biomagnification of a chemical with the respective combination of log K_{OA} and log K_{OW} in that species. White space in the plot indicates chemical partition properties where biomagnification is not possible according to these models.

 This journal is © The Royal Society of Chemistry 2025

Open Access Article. Published on 18 irailak 2025. Downloaded on 2026/04/18 18:27:39.
This article is licensed under a Creative Commons Attribution 3.0 Unported Licence.

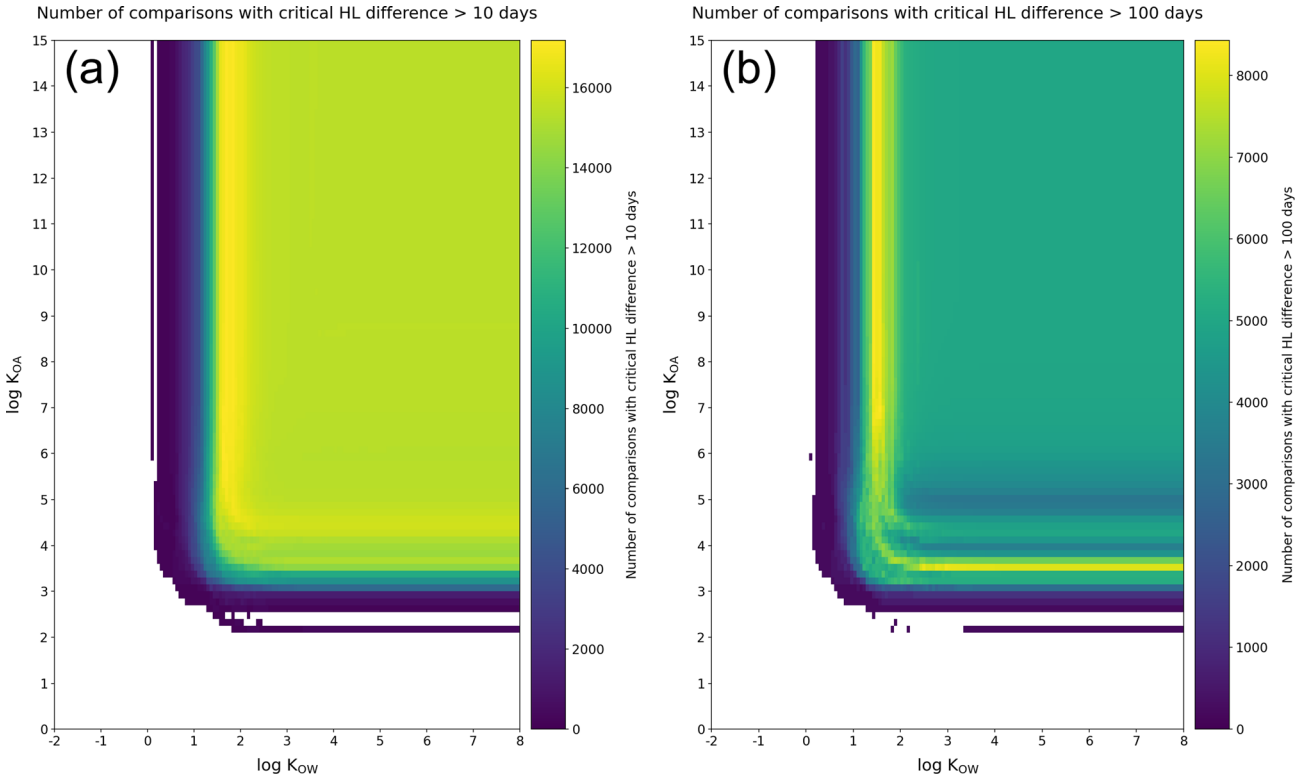

Fig. 2 Contour plots of the frequency of critical half-life values being >10 days (a) or >100 days (b) within partition space. Calculated with model 3 (model normalised, all K_{OW}) as how often this occurs for a given combination of log K_{OW} and log K_{OA} in a comparison of all species *vs.* all species. Yellow areas indicate chemical properties where large species differences occur most often.

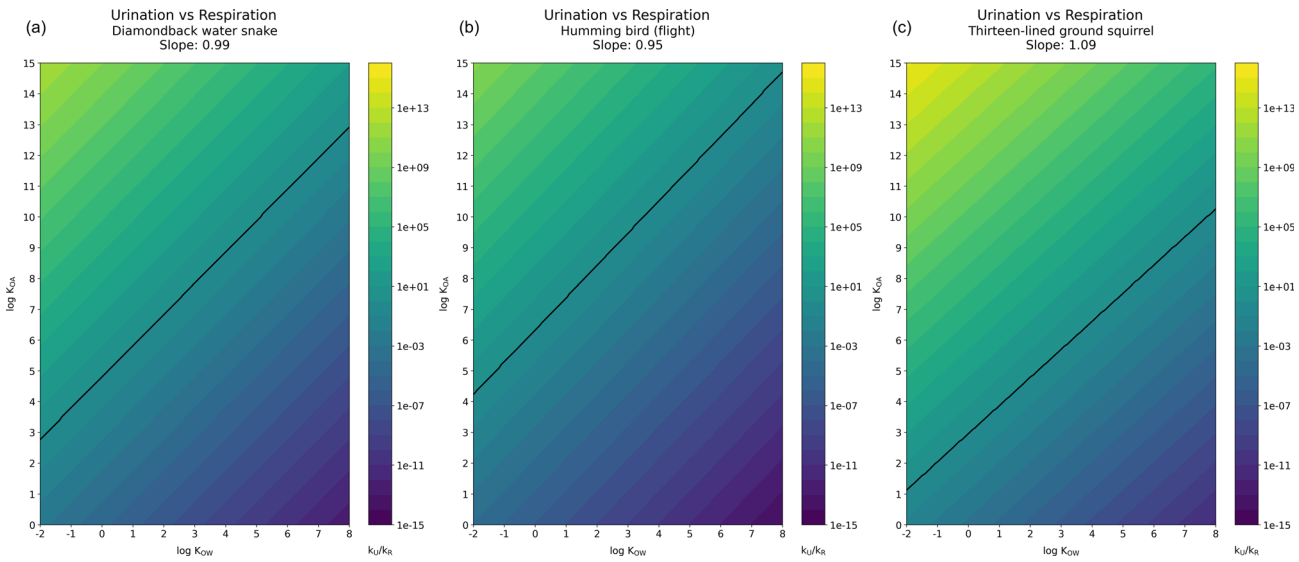

Fig. 3 Capacity to eliminate *via* urination (k_U) divided by the capacity to eliminate *via* respiration (k_R) plotted in chemical partition space. This ratio indicates which elimination pathway dominates in the absence of other elimination pathways. Chemicals with a combination of log K_{OA} and log K_{OW} above the black line (line indicates: $k_U/k_R = 1$) are predominantly eliminated *via* urination. See SI for 203 such plots.

than 4, partitioning into the different phases (*e.g.* water, protein, lipids) is important and that is why the model predictions differ here because the different normalisation terms become relevant. Second, the large model differences appear to also be more frequent for chemicals with log K_{OA} approximately between 3 and 5 in combination with a log K_{OW} greater than 2. This could be due to many species not biomagnifying in this area of partition space at all, hence the high frequency of model

Open Access Article. Published on 18 irailak 2025. Downloaded on 2026/04/18 18:27:39.
This article is licensed under a Creative Commons Attribution 3.0 Unported Licence.

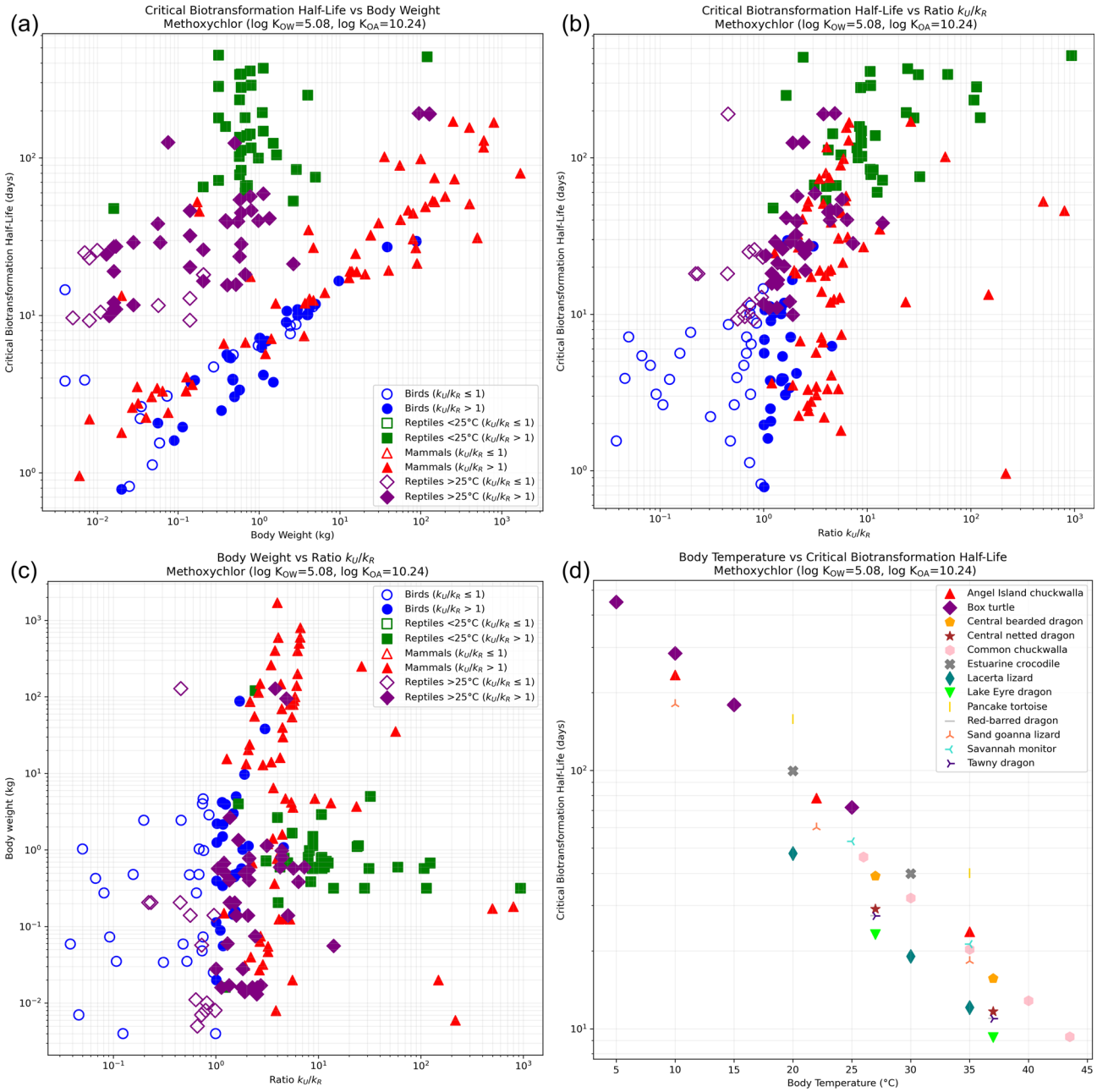

Fig. 4 Critical biotransformation half-life *vs.* body weight (a), critical biotransformation half-life *vs.* the ratio of k_U/k_R (b), body weight *vs.* the ratio of k_U/k_R (c) and critical biotransformation half-life *vs.* body temperature (d). Each data point represents a different dataset in panels (a)–(c), on log–log scale, symbols indicate different animal categories and whether elimination is dominantly *via* urination (full symbols) or respiration (open symbols). Panel (d) shows reptiles at different body temperatures (note: *y*-axis on log scale, *x*-axis on normal scale). All data is for the example of methoxychlor (CAS 72-43-5).

differences in an all-species *vs.* all-species comparison, and this same effect could also explain the first pattern of frequent model differences along the vertical axis. Out of all 20 503 comparisons 17 184 (84%) identified differences greater than 10 days and in 8431 (41%) comparisons the difference in the critical half-life was greater than 100 days. In other words: in the partition space analysed (15 251 chemicals, log K_{OW} −2 to 8, log K_{OA} 0 to 15, log unit grid matrix of size 101 × 151) there was at least one chemical for which the critical biotransformation half-life values differed by at least 100 d for 41% of species-by-species comparisons.

The methoxychlor case study provides further insights into species differences for one example chemical. Table 1 shows the species with the smallest and largest critical half-lives in each animal category (birds, mammals, reptiles <25 °C, reptiles >25 °C). In all four animal categories the differences in critical half-lives were at least one order of magnitude (Table 1), with the largest difference for mammals where critical half-lives spanned from 1 day to 171 days. This means that a conclusion about

 This journal is © The Royal Society of Chemistry 2025

Open Access Article. Published on 18 irailak 2025. Downloaded on 2026/04/18 18:27:39.
This article is licensed under a Creative Commons Attribution 3.0 Unported Licence.

Table 1 Selection of critical half-life values and the ratio of elimination *via* urination *vs.* respiration (k_U/k_R) for methoxychlor (CAS 72-43-5, log K_{OW} 5.08, log K_{OA} 10.244, both at 25 °C) as example. Shown are the species with the smallest and largest values in each animal category. The laboratory rat is also shown for comparison. Critical biotransformation half-lives calculated with model 3. Allometric and temperature scaling following the approach provided in the BAT user manual (page 22).[24]

Animal	Category	k_U/k_R	Body weight [kg]	Body temperature [°C]	Critical biotransformation half-life [d]	Critical biotransformation half-life scaled by weight [d], scaled to 1 kg	Critical biotransformation half-life scaled by weight and temperature [d], scaled to 1 kg & 25 °C
Species with minimum and maximum critical half-lives							
House finch	Birds	1.009	0.02	41.25	7.87×10^{-1}	2.09×10^{0}	2.46×10^{0}
Ostrich	Birds	1.698	88	40	2.96×10^{1}	9.65×10^{0}	1.12×10^{1}
Little brown bat (hibernation)	Mammals	216.5	0.006	37	9.59×10^{-1}	3.45×10^{0}	3.89×10^{0}
Florida manatee	Mammals	26.33	250	35.4	1.71×10^{2}	4.30×10^{1}	4.77×10^{1}
Lacerta lizard (a)	Reptiles <25 °C	1.235	0.016	20	4.77×10^{1}	1.34×10^{2}	1.27×10^{2}
Box turtle (a)	Reptiles <25 °C	936.6	0.316	5	4.49×10^{2}	5.99×10^{2}	4.91×10^{2}
Lake eyre dragon (b)	Reptiles >25 °C	0.795	0.008	37	9.26×10^{0}	3.10×10^{1}	3.49×10^{1}
Green sea turtle (c)	Reptiles >25 °C	4.862	94.5	27.5	1.93×10^{2}	6.18×10^{1}	6.34×10^{1}
Species with minimum and maximum ratio k_U/k_R							
Evening grosbeak (flight)	Birds	0.038	0.059	40	1.55×10^{0}	3.14×10^{0}	3.65×10^{0}
Little penguin	Birds	4.567	1.082	40	6.24×10^{0}	6.12×10^{0}	7.11×10^{0}
Egyptian fruit bat	Mammals	1.197	0.15	36.53	3.62×10^{0}	5.82×10^{0}	6.53×10^{0}
Thirteen-lined ground squirrel	Mammals	797.7	0.183	7.6	4.58×10^{1}	7.00×10^{1}	5.88×10^{1}
Lacerta lizard (a)	Reptiles <25 °C	1.235	0.016	20	4.77×10^{1}	1.34×10^{2}	1.27×10^{2}
Box turtle (a)	Reptiles <25 °C	936.6	0.316	5	4.49×10^{2}	5.99×10^{2}	4.91×10^{2}
Green iguana (c)	Reptiles >25 °C	0.221	0.206	34	1.82×10^{1}	2.69×10^{1}	2.95×10^{1}
American alligator (b)	Reptiles >25 °C	14.09	0.056	27	3.82×10^{1}	7.85×10^{1}	8.01×10^{1}
Laboratory rat for comparison							
Sprague-dawley rat	Mammal	3.737	0.365	37	6.62×10^{0}	8.51×10^{0}	9.60×10^{0}

the likelihood of biomagnification based on a single half-life for a standard laboratory animal such as the rat is difficult to extrapolate to the diversity of wildlife. A large portion of those inter-species differences can be explained by differences in body weight and temperature. The last two columns of Table 1 show the critical biotransformation half-lives scaled to a 1 kg organism with body temperature 25 °C. After scaling the critical biotransformation half-lives differ much less, with the largest difference for birds being reduced from a factor of 38 for unscaled maximum differences to 5 after scaling and similar reductions from factor 178 to 12 for mammals, from factor 9 to 4 for reptiles <25 °C and from factor 21 to 2 for reptiles >25 °C.

Fig. 4a further illustrates that the differences between species are not easily explained by body weight differences alone because the range of critical biotransformation half-lives for a given body weight can span several orders of magnitude across different species, although the two variables correlate (Spearman rank correlation coefficient on log transformed data (r_s) = 0.756, $P = 1.15 \times 10^{-12}$). This correlation is strongest for birds ($r_s = 0.806$, $P = 3.38 \times 10^{-13}$) and mammals ($r_s = 0.886$, $P = 2.20 \times 10^{-22}$), and strong for reptiles > 25 °C ($r_s = 0.601$, $P = 3.91 \times 10^{-6}$), whilst absent for reptiles < 25 °C ($r_s = 0.072$, $P = 6.77 \times 10^{-1}$). The correlation for reptiles >25 °C is strongly influenced by the two data points with the largest body weight, which are both for the green see turtle. The correlations between critical biotransformation half-lives and body weight are all, at least in part, a consequence of the use of allometric scaling to derive animal feeding and urination rates. The variation in critical half-lives for a given body weight is generally less than one order of magnitude for birds above 0.1 kg body weight and it is also less variable for mammals compared to reptiles (Fig. 4a). The greater variation in critical biotransformation half-lives for species with similar weight that is apparent in the reptile data can be attributed to the influence of temperature correction on feeding and urination rates for these ectothermic animals. The relationship between critical half-lives and body weight can be useful to approximate critical half-lives from body weight in the absence of further data, but the reliability of the species-specific model predictions is much greater.

There is also a correlation between the critical biotransformation half-lives and the ratio of elimination *via* urination over respiration (k_U/k_R, Fig. 4b, $r_s = 0.628$, $P = 1.12 \times 10^{-23}$). The relationship between body weight and the ratio of elimination *via* urination over respiration (k_U/k_R) is less strong (Fig. 4c, $r_s = 0.333$, $P = 1.17 \times 10^{-6}$). Both relationships originate in part

Open Access Article. Published on 18 irailak 2025. Downloaded on 2026/04/18 18:27:39.
This article is licensed under a Creative Commons Attribution 3.0 Unported Licence.

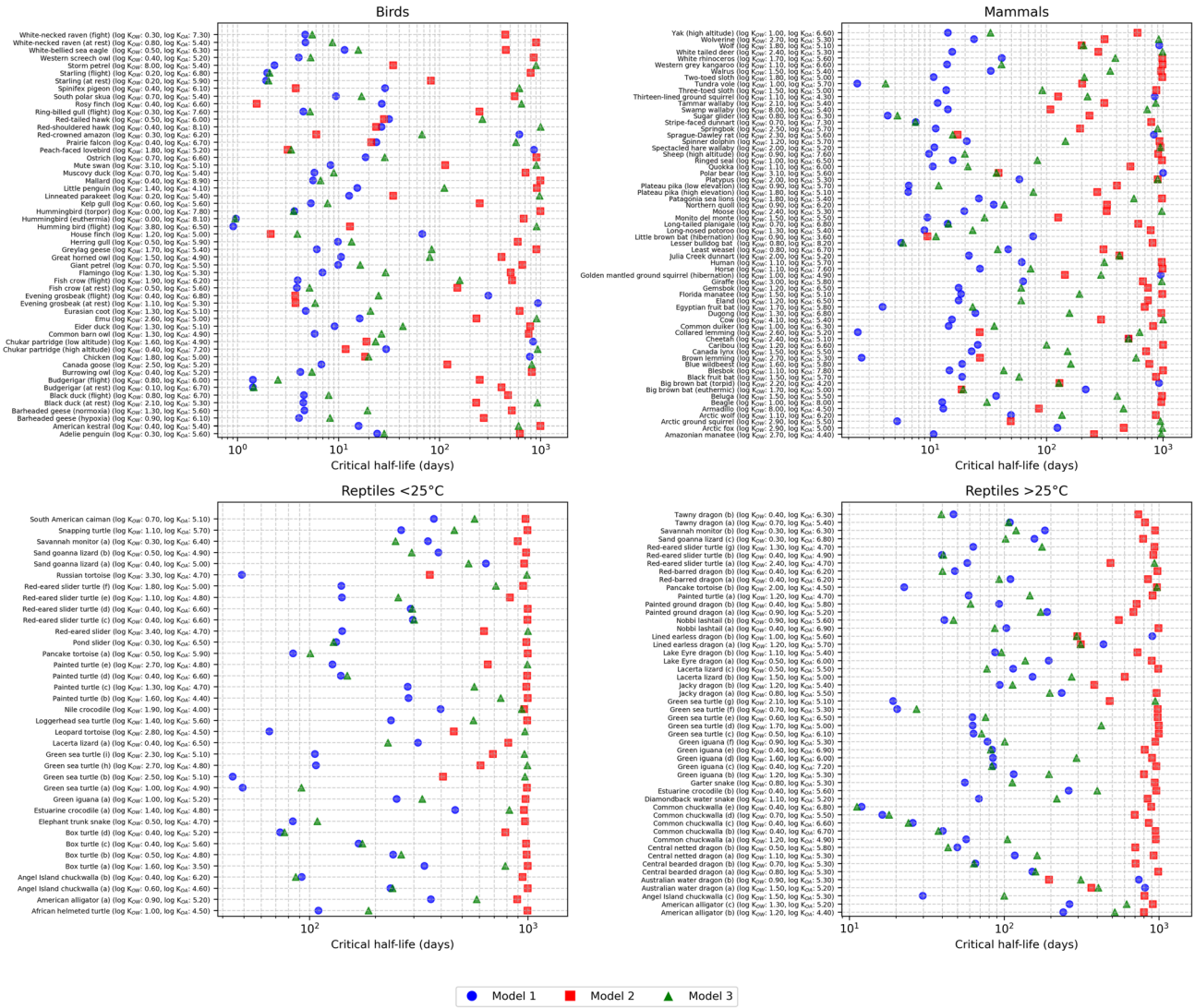

Fig. 5 Model differences in critical biotransformation half-lives. Shown are the values for the three models at the combination of log K_{OW} and log K_{OA} where the largest difference between any of the three models occurs for a given species. This analysis was restricted to critical half-lives between 0.1 and 1000 days.

from the allometric scaling used to derive the urination rate constant. This does not mean they are artificial, but it means that we are looking at indirect evidence for these relationships, subject to the assumption that the allometric relationships for urination rates are reliable.

An analysis of the reptiles with parameterisations at different temperatures, for the example methoxychlor, (Fig. 4d), shows a log-linear relationship between critical half-lives and body temperatures. The critical half-lives decline with increasing body temperature and Fig. 4d shows an approximately factor 2.5 reduction in the critical biotransformation half-life for a 10 °C increase in body temperature. The relationship is very close to the Q_{10} temperature correction (factor 2.5 per 10 °C) applied to the urination rates and field metabolic rates (which in turn influence feeding rates) by Saunders & Wania[9] (*i.e.* the model input data used here). The temperature correction of K_{OA} indirectly influences the elimination *via* respiration, which is further complicating the interpretation of what part of the model is responsible for the observed pattern.

Critical biotransformation half-lives: differences between models (normalisation)

Furthermore, the shape and contours of that partition space depend on the model used (*e.g.* Fig. 1d–f). Also, when using the same model, the shape of the critical chemical partition space differs from species to species (*e.g.* compare Fig. 1c *vs.* 1f *vs.* 1i). Different BMF model choice can lead to slightly larger or smaller portions of the chemical partition space where biomagnification is possible at all (*e.g.* compare Fig. 1d–f) as well as different hotspots where the fastest biotransformation rates are required to avoid biomagnification (*e.g.* compare Fig. 1e *vs.* 1f).

To better understand the magnitude of model differences I selected the combination of log K_{OW} and log K_{OA} for each

Open Access Article. Published on 18 irailak 2025. Downloaded on 2026/04/18 18:27:39. This article is licensed under a Creative Commons Attribution 3.0 Unported Licence.

species where the differences in critical half-lives were greatest amongst the three models (largest differences between any of the three models in a three-way-comparison). This analysis was restricted to critical half-lives between 0.1 and 1000 days for any of the three models because that is the range of practical interest. The results are shown in Fig. 5. In all four animal categories the maximum difference is very large, typically about two orders of magnitude, and for each species the maximum difference occurs at different combinations of $\log K_{OW}$ and $\log K_{OA}$. Generally, and across all data, model 1 tends to predict shorter critical half-lives and model 2 tends to predict the longest, whilst model 3 predictions tend to fall in between. However, for individual species the order of the models can differ. All these model differences (*e.g.* Fig. 5) are due to the normalisation terms (or lack of in model 1) and they can result in large differences between the predicted critical biotransformation half-lives.

Implications of model differences due to normalisation

The BMF is defined as the ratio of two concentrations in different media (prey and predator) with different compositions and normalisation is required to make them comparable. The simulations in this study have shown that the choice of normalisation or lack thereof can have a big influence on the critical biotransformation half-life in partition space and that this effect varies from species to species. This means that when using a BMF model to assess the likelihood of biomagnification it matters very much which normalisation is used. For one normalisation a given measured half-life of a compound would be interpreted as evidence that no biomagnification occurs whereas for a different normalisation the opposite conclusion would be drawn. And where exactly this error occurs is different for each species modelled (Fig. 5). Thus, the use of normalised or not normalised data and models can be a source of confusion, because the same chemical would either be classed as biomagnifying or not biomagnifying, depending on which normalisation is used. Thus, the use of normalisation must be carefully considered. We also need a better understanding of what the critical biotransformation half-lives mean when they are calculated with a model that uses normalisation. Or putting it differently: we need to clarify how measured or predicted biotransformation half-lives should be used in BMF models that use normalisation. What does this mean for chemical assessment and regulatory use of such models? I believe further investigation and discussion of this aspect is needed.

Factors influencing critical biotransformation half-lives

Goss *et al.*[19] hypothesised that the critical elimination half-life to avoid biomagnification could be roughly constant for different species if allometric scaling co-varies in such a way that differences in rates of elimination *via* one pathway are compensated by corresponding changes in other pathways. Although the critical elimination half-life defined by Goss *et al.* is different to the critical biotransformation half-life used here, a similar hypothesis could be proposed about critical biotransformation half-lives. However, this study clearly shows that critical biotransformation half-lives vary from species to species and that allometric differences in urination and respiration do not co-vary in such a way that a critical biotransformation half-life emerges for a given chemical that is constant across different species (Fig. 4, 5 and Table 1). Apart from the methoxychlor case study results shown in Fig. 4, 5 and Table 1, this can also be seen from the species-by-species differences in the contours of the critical half-lives (Fig. 1 and corresponding Fig. in SI folder "SI HL contour plots"), or in the areas where urination or respiration dominate elimination in partition space (Fig. 3 and corresponding Fig. in SI folder "SI Fig. U *vs.* R with slopes") as well as the methoxychlor case study (Fig. 4).

Fig. 3 and the corresponding Fig. in the SI demonstrate that the predominant route of elimination for a given chemical can be different in different species and that for most chemicals one route dominates elimination in our model, which only considers two routes of elimination (urination, respiration). When more routes are considered, they likely dominate in different parts of the chemical partition space as shown by Lee *et al.* for rats.[26]

Critical biotransformation half-lives and dominant elimination pathways differ substantially from species to species (Fig. 1, 3 and 4) and these differences also vary on a chemical-by-chemical basis which can be seen from the differences in the contours of the chemical partition space plots (Fig. 1–3 and in SI). All this means that an accurate assessment of the potential bioaccumulation and biomagnification of chemicals in food-chains requires calculations for each species and importantly, for each food-chain, separately. Single cut-off values for K_{OA} and K_{OW} likely lead to frequent false positive and false negative classifications of chemicals as biomagnifying.

Dominant elimination route

The models further enable a deeper understanding of which elimination route is most relevant for different chemicals in the absence of biotransformation (*e.g.* Fig. 3, all Fig. in SI folder "SI Fig. U *vs.* R with slopes"). When plotting the ratio of the capacity to eliminate *via* urination (k_U, rate constant for excretion *via* urination) and the capacity to eliminate *via* respiration (k_R, rate constant for excretion *via* respiration) a value above 1 (above the black line in Fig. 3) indicates areas of chemical partition space where urination is the predominant route of elimination and values below 1 indicate that elimination occurs predominantly *via* respiration. The position of this line of separation between elimination pathways differs substantially between different species (Fig. 3, also see all plots in SI) and the slope of that line can also differ (*e.g.* Fig. 3), ranging from 0.9011 to 1.1106 across all datasets.

In the methoxychlor case study lower critical biotransformation half-lives are generally associated with lower ratios of k_U/k_R (Fig. 4 and Table 1). This chemical is more likely to biomagnify through food-chains with species that eliminate methoxychlor predominantly *via* respiration (*i.e.* species with little urination) and because methoxychlor has a relatively high $\log K_{OA}$ value (weak partitioning into air) this elimination

Open Access Article. Published on 18 irailak 2025. Downloaded on 2026/04/18 18:27:39. This article is licensed under a Creative Commons Attribution 3.0 Unported Licence.

pathway is insufficient. In those cases, biomagnification occurs unless biotransformation eliminates the chemical.

Modelling bioaccumulation in food-chains

Modelling bioaccumulation in food-chains may be motivated by different aims. One is the classical purpose of identifying persistent organic pollutants. For this regulatory purpose, it is important to identify biomagnifying chemicals and this requires normalisation to meet the definition of biomagnification in this context.[4] Approaches recommended in regulatory guidance for lower tiers and screening purposes are typically based on generic cut-off values, for example those used in the REACH PBT regulation.[13,14] These inherently accept a lower accuracy to identify chemicals that biomagnify in real food-webs at the lower, screening tiers, because higher tier approaches allow for more realistic and accurate assessments. This suggests that such higher tier approaches are available, but they are currently limited to laboratory species (*e.g.* rat) rather than relevant food-chain species.

The normalisation approach is well accepted in bioaccumulation studies, particularly in field and modelling studies that derive bioaccumulation metrics in air-breathing wildlife. Calculating bioaccumulation metrics is one aim. Another aim is to calculate concentrations of chemicals, *e.g.* plant protection products, in top-predators so that those predicted body residues can be compared with thresholds for toxic effects in a risk assessment and this purpose may not require normalisation in the model or a different approach altogether depending on the mode of action of the toxicant and where its target site is located in the animal. In this case it may be better to use physiologically based pharmacokinetic models to calculate the biologically active dose at the target sites in the laboratory test organism as well as the wildlife animal of concern at the end of the food-chain. If the target site is not in a lipid phase, then lipid-normalised body-residues may be misleading. And because this study has shown the substantial influence of different normalisation approaches applied to the BMF model it is important to carefully consider when to use a normalisation approach for the purposes of environmental risk assessment and which type of normalisation.

Building food-webs and food-chain models that are more realistic for specific groups of chemicals, *e.g.* plant protection products, is one way of increasing the accuracy of biomagnification assessment. The substantial species-by-species differences in biomagnification shown here and previously[9] suggest that there will be substantial differences in the predicted concentrations in top predators of different food-chains in different ecosystems, simply due to the differences in the species present in those food chains. This very likely also translates to different conclusions about whether a given chemical is biomagnifying, depending on which food-chain is modelled.

Biotransformation and weight of evidence approaches

A weight of evidence approach has been proposed for evaluating the bioaccumulation and biomagnification of chemicals[17] and a software tool (Bioaccumulation Assessment Tool [BAT] in EAS-E-Suite) is available for that purpose.[24] Biotransformation rates and half-lives can be entered for any species for which data is available, and this is then used to calculate bioaccumulation and biomagnification metrics for the species in the food-webs implemented in the BAT tool. Biotransformation rates are extrapolated between species using allometric scaling (p 22, BAT user manual[24]). The problem is that the predictive validity of this allometric scaling of biotransformation rates between species is unknown. This structural model uncertainty is currently difficult to quantify because we do know biotransformation rates or half-lives for only very few species and chemicals. For this reason, it is also difficult to reduce this uncertainty by building improved models for extrapolation of biotransformation between species. Unless substantially more data on biotransformation in wildlife becomes available this situation is unlikely to change and modelling of bioaccumulation and biomagnification in wildlife will remain highly uncertain.

In my view, the uncertainty around biotransformation in different species is the greatest source of uncertainty in the assessment of bioaccumulation and biomagnification and for this reason I propose a slightly different weight of evidence approach. Instead of calculating bioaccumulation and biomagnification factors associated with great and unknown uncertainty, I suggest that it is better to calculate the critical biotransformation half-life in the species of concern and then compare that critical biotransformation half-life to available biotransformation data. This biotransformation data can cover different species and originate from *in vivo*, *in vitro* or *in silico* studies. By comparing biotransformation half-lives side by side with the critical values required to avoid biomagnification the assessor can make a judgement on the likelihood of biomagnification to occur. The discrepancy of biotransformation data coming from different species is laid open and made transparent. This is the main difference to the weight of evidence approach in the BAT and elsewhere (incl. Table 1 of this study), where biotransformation is extrapolated between species with unknown, but likely very large uncertainty and unknown predictive validity. My proposed weight of evidence assessment on biotransformation half-lives eliminates the need to include this extrapolation in model calculations. Instead, the greatest source of uncertainty, extrapolation of biotransformation between species, is clearly brought into the focus of the expert judgement.

Illustrative example of weight of evidence approach

I illustrate the proposed weight of evidence approach using the chemical methoxychlor (CAS 72-43-5) and a hypothetical, illustrative food-chain as an example. This food-chain consists of the tundra-vole (*Microtus oeconomus*), which, for this illustration, is assumed to consume plant material with chemical residues, and its predator, the red-tailed hawk (*Buteo jamaicensis*).

A weight of evidence assessment to answer the question if methoxychlor would biomagnify in this hypothetical,

Open Access Article. Published on 18 irailak 2025. Downloaded on 2026/04/18 18:27:39. This article is licensed under a Creative Commons Attribution 3.0 Unported Licence.

illustrative food-chain now requires judging the likelihood of biotransformation half-lives in the food-chain species (vole, hawk) to be below the threshold values of the critical whole-body biotransformation half-life – given the data on other species, derived using a variety of methods. This judgement requires considering the phylogenetic relationship of the species, their size, the type of data (*e.g. in vitro* or *in vivo*) and other factors. A challenge and typical problem are that some of the available data is usually for liver only whereas the biomagnification models require whole-body biotransformation data. The mismatched types of data are still useful, but not the most appropriate for this type of simple one-compartment model (*e.g.* in contrast to physiologically-based pharmacokinetic models).

The critical biotransformation half-life in the rat is 12.2 days for methoxychlor (model 1) and comparing this value with the *in vitro* half-lives available for the rat, shows that there would be likely no biomagnification in the rat (Table 2). The comparison with the required critical half-lives for the tundra-vole (1.20 days) and the red-tailed hawk (4.35 days) shows that the tundra-vole and the red-tailed hawk are more susceptible to biomagnification of this compound than the rat, because they require shorter biotransformation half-lives than the rat to avoid biomagnification of methoxychlor. The rat is, however, not the closest relative of the hawk for which data is available and therefore perhaps less relevant. The *in vitro* half-life measured in quail is about 19 times shorter than the critical half-life in the hawk and this may again be viewed as a sufficient margin of safety to conclude that biomagnification is unlikely in the hawk in this case. The fish data in Table 2 provides further context and a good example of the inherent variability and uncertainty in biotransformation data, because the two half-life estimates for fish, one estimated *in silico* and the other measured *in vitro* differ by a factor of 147, which I take as a sign to be sceptical and cautious when extrapolating from *in vitro* to whole-organism biotransformation half-lives. I refrain from a final judgement on the likelihood of biomagnification in this illustrative food-chain because it is not the aim of this study to provide an actual assessment of the biomagnification potential of methoxychlor. An actual assessment would also need to include appropriate, quantitative *in vitro* to *in vivo* extrapolation, which was beyond the scope of this study and would require substantial research for many relevant wildlife taxa.

The aim here is to illustrate and advocate for assessing critical biotransformation half-life values in a weight of evidence. What becomes obvious from this presentation (Table 2) is the wide range of relevant half-life data, which represents both, variability and uncertainty. Sources of variability are species differences and inherent biological variability within the different test systems. Uncertainty originates from knowledge gaps in the *in vitro* to *in vivo* extrapolation, measurement errors as well as lack of measurements of the actual parameter of interest. The lack of data for the exact species in the food-chain and the diversity of methods to derive half-lives (*e.g. in silico*, *in vitro*) are typical. This makes the weight of evidence assessment challenging, but still a lot more tractable than trying to aggregate this data into a single half-life value for each food-chain species to calculate BMF values explicitly. The propagation of variability and uncertainty in model input parameters through to the model prediction is technically challenging, because the distributions of input parameters are difficult to characterise and often unknown. Accurate probabilistic predictions are also essentially impossible if the covariation structure between different inputs is unknown, as is currently the case for the BMF model. The study by Wania *et al.*[28] is informative in this context, because they identified chemicals likely to bioaccumulate in air-breathing organisms using predicted biotransformation half-lives and concluded

Table 2 Illustrative example of a weight of evidence assessment of potential biomagnification in a two-species food-chain. The example chemical is methoxychlor (CAS 72-43-5, log K_{OW} 5.08, log K_{OA} 10.244). Critical biotransformation half-lives are calculated with the kinetic model (model 1). Note that some data are for whole-body biotransformation and some for liver only

Type of half-life	Value [d]	Species	Notes	Source
Critical whole-body biotransformation half-life	**1.20×10^{0}**	**Tundra-vole**	Kinetic BMF model, eqn (4)	This study
Whole-body biotransformation half-life	1.05×10^{-2}	Rat	Extrapolated from depletion assays in rat liver S9 fractions	26
Half-life in liver *in vitro*	6.66×10^{-2}	Rat	Calculated from loss of ^{14}C labelled parent after 2 h in liver slices *in vitro*	27
Half-life in liver *in vitro*	3.10×10^{-1}	Mouse	Calculated from loss of ^{14}C labelled parent after 2 h in liver slices *in vitro*	27
Predicted whole-body biotransformation half-life	5.99×10^{0}	Human	Predicted from molecular structure using a qsar	25
Critical whole-body biotransformation half-life	**4.35×10^{0}**	**Red-tailed hawk**	Kinetic BMF model, eqn (4)	This study
Half-life in liver *in vitro*	2.21×10^{-1}	Quail	Calculated from loss of ^{14}C labelled parent after 2 h in liver slices *in vitro*	27
Predicted whole-body biotransformation half-life	2.71×10^{1}	Fish	Predicted from molecular structure using a qsar	25
Half-life in liver *in vitro*	1.84×10^{-1}	Trout	Calculated from loss of ^{14}C labelled parent after 2 h in liver slices *in vitro*	27

Open Access Article. Published on 18 irailak 2025. Downloaded on 2026/04/18 18:27:39. This article is licensed under a Creative Commons Attribution 3.0 Unported Licence.

that the reliability of their method depends strongly on the accuracy of the biotransformation prediction, which is very uncertain. Assessing critical biotransformation half-lives directly, as proposed here, does not completely avoid that issue, but makes it transparent and subject to explicit expert judgement.

Allometric scaling as model limitation and source of uncertainty

Above I have argued that allometric scaling is a source of uncertainty and that this uncertainty can be reduced by a weight of evidence assessment of biotransformation data (Table 2). However, this perspective ignores the fact that the models used here to calculate the critical biotransformation half-lives implicitly also rely on allometric scaling. This is because for many species it is difficult to find the values of the required model parameters, such as for example the rates of feeding, respiration and urination or the fractional proportions of lipid, protein and carbohydrates in their body and diets. These missing values are often read-across from different species or estimated from different species using allometric scaling, including in the current dataset from Saunders & Wania.[9] Here, allometric scaling was used in the derivation of the animal feeding and urination rates and therefore influences both, the numerator and the denominator of the biomagnification model (eqn (1) and (2)).

Another aspect is the comparison of *in vitro* biotransformation data with whole-body critical biotransformation half-lives. Above I have simply argued that expert judgment is required in this comparison, however a more rigorous approach would be to formally perform a quantitative *in vitro* to *in vivo* extrapolation. Such calculations would then again most likely rely on allometric scaling for some of the required physiological parameters (*e.g.* blood flow to liver).

Furthermore, I have used allometric scaling and temperature correction (eqn (12)) to convert critical biotransformation half-lives from species-specific values to values for a hypothetical animal with body weight 1 kg and body temperature 25 °C in Table 1. After conversion the critical biotransformation half-lives differ less and this reduction in differences can be interpreted as the part that is due to different body size and temperature in the species-specific values. This insight is useful, but it rests on the assumed reliability of eqn (12). The reliability of this equation is unknown because we generally lack data on measured biotransformation in diverse wildlife. Although there is evidence from ecology supporting that rate constants generally decrease with body weight at an exponent of −0.25,[29] the evidence, theory and applicability to chemical clearance are subject to intense scientific debate.[30] And, whilst there is evidence that muscle metabolic enzyme activity scales with body weight,[31] it is a strong assumption to expect the same for xenobiotic biotransformation rates. In eqn (12) body weight scaling and temperature correction of biotransformation rates are treated independently, whilst there is some evidence of an interaction of the allometric scaling of metabolic rates and temperature.[30,32] Increasing availability of biotransformation rates measured at different temperatures will also enable better characterisation of the temperature dependence of biotransformation.[33]

Generally, there is more data available on feeding, respiration and urination rates to build allometric relationships than is for biotransformation rates in different species. There is a vast number of allometric relationships available, with slightly different exponents and important differences in the taxa included in the underlying data. Future food-chain models could be made more reliable by ensuring that the species included are within the applicability domain of allometric relationships used (*i.e.* taxa).

Thus, when we calculate BMF values or critical biotransformation half-lives, allometric scaling can be helpful or even necessary for many purposes: to extrapolate measured biotransformation half-lives from one species to another, to estimate species parameters such as feeding, respiration or urination rates to be used as model parameters, to perform *in vitro* to *in vivo* extrapolation. However, the reliability of these approaches is difficult to assess and a subjective judgement. More research to quantify the uncertainty and reliability of these applications of allometric scaling to biomagnification assessment would help to better select the best approach.

Contour plots in partition space

Contour plots in partition space have been popular in the assessment of bioaccumulation and biomagnification. However, there is no agreement on what metric should by plotted in the *z*-dimension. The main school of thought plots BMF values in partition space,[1,2,15,34,35] proportion of species with BMF below one,[9] and calculated trophic magnification factors in food-webs.[34] The problem with this approach is that it requires either to assume zero biotransformation or to plot multiple partition space plots, one for each assumed biotransformation rate or half-life.[26,35] This problem is avoided when plotting half-lives in partition space as first proposed by Goss *et al.*[19] using elimination half-lives in human as example. Goss *et al.* also provide several theoretical reasons why half-lives are better suited for assessing the bioaccumulation potential of chemicals.

The steady-state model assumption

The origin of the BMF models and concepts is in studies on persistent organic pollutants (POPs) and some of the assumptions that were appropriate for POPs are likely not valid for other classes of chemicals, for example modern plant protection products. Most important is the assumption of steady-state, which means that the chemical is assumed to be at steady-state distribution between different environmental media (*e.g.* soil, plants, air, water, biota) and that the concentrations in these compartments do not change over time. This is unlikely to be the case for chemicals that degrade in the environment (*e.g.* in soil, water and air) and are emitted only intermittently instead of continuously. Under non-steady state conditions, it becomes more important to also consider seasonal variations of diets and food-webs as well as spatial variation in exposure (home-ranges, foraging ranges) when trying to estimate the likelihood of biomagnification along food-

 This journal is © The Royal Society of Chemistry 2025

Open Access Article. Published on 18 irailak 2025. Downloaded on 2026/04/18 18:27:39. This article is licensed under a Creative Commons Attribution 3.0 Unported Licence.

chains. It is also important to note, that the dataset used here comprises multiple entries for the same species in a few cases and the differences include at flight *vs.* at rest, hibernating *vs.* not hibernating, torpor *vs.* euthermia, high altitude *vs.* low altitude and different body temperatures. Animals are rarely at steady-state and the simplified steady-state representation of animals by the models, using static parameterisations, is a limitation. Non-steady state (dynamic) biomagnification models are more realistic and this requires dynamic parametrisation of the models. The different critical half-lives derived for the same species in different states (different parameterisations) need to be interpreted together because if the actual biotransformation half-life lies between those values it would mean that the animal would temporarily biomagnify and at other times it would not. Taking a simple average of the critical half-lives may again be an over-simplification because different animal states may be more relevant for food-chain biomagnification than others (*e.g.* depending in which state animals eat or become prey). Also the capacity to biotransform may vary depending on energy intake[36] and demand (*e.g.* rest *vs.* flight, active *vs.* hibernation), which is why integration of biomagnification modelling with dynamic energy budget theory[37,38] may be helpful. The overall result can be modelled using dynamic simulations, including dynamic food-chain simulations. This suggests that the steady-state BMF modelling approach may need to be refined in future work using dynamic models.

Limited species coverage, phylogeny, difficulty of validation and further limitations

Limitations in the currently used models are their limited number of species included and that those species are often not relevant for chemicals other than POPs. For example, arctic food-chains like the lichen-caribou-wolf food chain[1,17] are of little relevance to agricultural ecosystems, whereas the classical grass-cow food chain is an example to the contrary.[2,39] In summary, the representation of the animal kingdom in current BMF models is very poor, we now know that species differ substantially in their biomagnification processes,[9] and taken together this means that we need more realistic and representative models to assess the biomagnification potential of chemicals that are not at environmental steady-state, *e.g.* modern plant protection products.

This study, based on the work of Saunders & Wania,[9] grouped species into birds, mammals and reptiles. It is important to note that birds and mammals are relatively small, monophyletic groups, whilst the species grouped under reptiles here are a much more phylogenetically diverse group and more closely related to birds than mammals.[40] This is relevant, to keep in mind when interpreting the results of this study (*e.g.* because different groups under 'reptiles' might differ in physiology[41]), but also because phylogeny may help predicting biotransformation capabilities across species.[42,43]

Further limitations are poor knowledge of the uptake efficiency of different chemicals from the gastrointestinal tract in different species and the lack of physiological data to parameterise more elimination pathways, besides respiration and urination, for more than a few well studied species (*e.g.* rat[26]). And even for those wildlife species where we can model the BMF we have very little data to validate the BMF models. Although these models are built on strong theoretical grounds and validation with field data has been done in some food-chains,[1] the general predictive validity beyond those food-chains and studied substances is unknown (see also[44]).

Conclusions

The critical biotransformation half-life is the maximum half-life to avoid biomagnification of a chemical. Shorter biotransformation half-lives do not result in biomagnification. Contour plots of critical biotransformation half-lives in partition space for different species make it very easy to understand which physical–chemical properties of chemicals make biotransformation in different species more or less likely. This analysis shows great inter-species differences in critical biotransformation half-lives. Species by species differences are substantial, relevant and greater than previously known, also and especially when applying different or no normalisation. When using BMF models to assess biomagnification potential, the conclusion for a chemical with a given measured biotransformation half-life can be contradictory, depending on which normalisation is used. BMF assessment is based on the ratio of two concentrations in different matrices and therefore requires normalisation. However, this study shows that applying different or no normalisation also results in very different critical biotransformation half-lives, which was previously unknown and of surprising magnitude.

Assessment of the biomagnification potential of chemicals needs to be made more realistic and accurate by building dynamic models for relevant food-chains and including a much greater diversity of species and more relevant species. Focussing on the biotransformation half-life as part of a weight of evidence assessment may currently be more tractable than predicting BMF values and can focus the attention on the greatest unknown: biotransformation half-lives of chemicals in wildlife.

Conflicts of interest

R. A. is currently affiliated to an organization (Syngenta) with a financial and non-financial interest in the subject matter discussed in this manuscript.

Data availability

The data supporting this article have been included as part of the SI. Supplementary information: chemical partition space plots showing critical half-lives (like Fig. 1) for 203 datasets and 3 models; chemical partition space plots showing urination *vs.* respiration rate constants (like Fig. 3) for 203 datasets; the input data file used to create these plots; the model code (Python) to recreate all figures and data in tables; the Python script to calculate critical half-life values for a single substance as used in the case study. See DOI: **https://doi.org/10.1039/d5em00220f**.

Open Access Article. Published on 18 irailak 2025. Downloaded on 2026/04/18 18:27:39. This article is licensed under a Creative Commons Attribution 3.0 Unported Licence.

Acknowledgements

I'm very grateful to Leslie Saunders and Frank Wania for publishing a comprehensive dataset of species parameters for biomagnification modelling with their excellent paper. I also thank Paul Whalley, Amund Løvik and Helen Thompson for very helpful suggestions on an earlier version of this manuscript. I also am very grateful for the constructive and thoughtful reviewer comments. This work has been funded by Syngenta Crop Protection AG.

References

1 B. C. Kelly, M. G. Ikonomou, J. D. Blair, A. E. Morin and F. A. P. C. Gobas, Food Web-Specific Biomagnification of Persistent Organic Pollutants, *Science*, 2007, **317**, 236–239.
2 G. Czub and M. S. McLachlan, Bioaccumulation Potential of Persistent Organic Chemicals in Humans, *Environ. Sci. Technol.*, 2004, **38**, 2406–2412.
3 J. P. Connolly and C. J. Pedersen, A thermodynamic-based evaluation of organic chemical accumulation in aquatic organisms, *Environ. Sci. Technol.*, 1988, **22**, 99–103.
4 F. A. P. C. Gobas, W. de Wolf, L. P. Burkhard, E. Verbruggen and K. Plotzke, Revisiting Bioaccumulation Criteria for POPs and PBT Assessments, *Integrated Environ. Assess. Manag.*, 2009, **5**, 624–637.
5 F. A. P. C. Gobas, J. B. Wilcockson, R. W. Russell and G. D. Haffner, Mechanism of biomagnification in fish under laboratory and field conditions, *Environ. Sci. Technol.*, 1999, **33**, 133–141.
6 F. A. P. C. Gobas, Gastrointestinal magnification: The mechanism of biomagnification and food chain accumulation of organic chemicals, *Environ. Sci. Technol.*, 1993, **27**, 2855–2863.
7 R. Macdonald, D. Mackay and B. Hickie, Peer Reviewed: Contaminant Amplification in the Environment, *Environ. Sci. Technol.*, 2002, **36**, 456A–462A.
8 F. A. P. C. Gobas, Y.-S. Lee and J. A. Arnot, Normalizing the Biomagnification Factor, *Environ. Toxicol. Chem.*, 2021, **40**, 1204–1211.
9 L. J. Saunders and F. Wania, Cross-Species Evaluation of Bioaccumulation Thresholds for Air-Breathing Animals, *Environ. Sci. Technol.*, 2023, **57**, 10491–10500.
10 A. M. H. deBruyn and F. A. P. C. Gobas, The sorptive capacity of animal protein, *Environ. Toxicol. Chem.*, 2007, **26**, 1803–1808.
11 C. E. Mackintosh, J. Maldonado, J. Hongwu, N. Hoover, A. Chong, M. G. Ikonomou and F. A. P. C. Gobas, Distribution of Phthalate Esters in a Marine Aquatic Food Web: Comparison to Polychlorinated Biphenyls, *Environ. Sci. Technol.*, 2004, **38**, 2011–2020.
12 D. Mackay and A. Fraser, Bioaccumulation of persistent organic chemicals: mechanisms and models, *Environ. Pollut.*, 2000, **110**, 375–391.
13 ECHA, *Chapter R.7c: Endpoint Specific guidance*, *Report ECHA-23-H-09-EN*, European Chemicals Agency, Helsinki, 2023.
14 ECHA, *Chapter R.11: PBT/vPvB Assessment, Report ECHA-23-H-10-EN*, European Chemicals Agency, Helsinki, 2023.
15 J. M. Armitage and F. A. P. C. Gobas, A Terrestrial Food-Chain Bioaccumulation Model for POPs, *Environ. Sci. Technol.*, 2007, **41**, 4019–4025.
16 B. C. Kelly, J. M. Sun, M. R. R. McDougall, E. M. Sunderland and F. A. P. C. Gobas, Development and Evaluation of Aquatic and Terrestrial Food Web Bioaccumulation Models for Per- and Polyfluoroalkyl Substances, *Environ. Sci. Technol.*, 2024, **58**(40), 17828–17837.
17 J. A. Arnot, L. Toose, J. M. Armitage, M. Embry, A. Sangion and L. Hughes, A weight of evidence approach for bioaccumulation assessment, *Integrated Environ. Assess. Manag.*, 2023, **19**, 1235–1253.
18 D. T. F. Kuo, B. A. Rattner, S. C. Marteinson, R. Letcher, K. J. Fernie, G. Treu, M. Deutsch, M. S. Johnson, S. Deglin and M. Embry, A Critical Review of Bioaccumulation and Biotransformation of Organic Chemicals in Birds, *Rev. Environ. Contam. Toxicol.*, 2022, **260**, 6.
19 K.-U. Goss, T. N. Brown and S. Endo, Elimination half-life as a metric for the bioaccumulation potential of chemicals in aquatic and terrestrial food chains, *Environ. Toxicol. Chem.*, 2013, **32**, 1663–1671.
20 J. A. Arnot, T. N. Brown and F. Wania, Estimating Screening-Level Organic Chemical Half-Lives in Humans, *Environ. Sci. Technol.*, 2014, **48**, 723–730.
21 F. A. P. C. Gobas, Y.-S. Lee, K. M. Fremlin, S. C. Stelmachuk and A. D. Redman, Methods for assessing the bioaccumulation of hydrocarbons and related substances in terrestrial organisms: A critical review, *Integrated Environ. Assess. Manag.*, 2023, **19**, 1433–1456.
22 Y. D. Lei, F. Wania, W. Y. Shiu and D. G. B. Boocock, HPLC-Based Method for Estimating the Temperature Dependence of n-Octanol–Water Partition Coefficients, *J. Chem. Eng. Data*, 2000, **45**, 738–742.
23 S. Baskaran, A. Podagatlapalli, A. Sangion and F. Wania, Predicting the Temperature Dependence of the Octanol–Air Partition Ratio: A New Model for Estimating $\Delta U^{\circ}OA$, *J. Solution Chem.*, 2023, **52**, 51–69.
24 J. M. T. Armitage, L. Toose, M. Embry, K. L. Foster, L. Hughes, A. Sangion and J. A. Arnot, *The Bioaccumulation Assessment Tool (BAT) Version 2.02*, ARC Arnot Research and Consulting Inc., Toronto, ON, Canada, 2021.
25 A. R. a. C. ARC, EAS-E Suite, **https://www.eas-e-suite.com**, accessed 20 January 2025.
26 Y. S. Lee, T. R. Cole, M. S. Jhutty, M. A. Cantu, B. Chee, S. C. Stelmaschuk and F. A. P. C. Gobas, Bioaccumulation Screening of Neutral Hydrophobic Organic Chemicals in Air-Breathing Organisms Using In Vitro Rat Liver S9 Biotransformation Assays, *Environ. Toxicol. Chem.*, 2022, **41**, 2565–2579.
27 K. Ohyama, S. Maki, K. Sato and Y. Kato, In vitro metabolism of [14C]methoxychlor in rat, mouse, Japanese quail and rainbow trout in precision-cut liver slices, *Xenobiotica*, 2004, **34**, 741–754.
28 F. Wania, Y. D. Lei, S. Baskaran and A. Sangion, Identifying organic chemicals not subject to bioaccumulation in air-

 This journal is © The Royal Society of Chemistry 2025

Open Access Article. Published on 18 irailak 2025. Downloaded on 2026/04/18 18:27:39.
This article is licensed under a Creative Commons Attribution 3.0 Unported Licence.

breathing organisms using predicted partitioning and biotransformation properties, *Integrated Environ. Assess. Manag.*, 2022, **18**, 1297–1312.

29 A. J. Hendriks, The power of size: A meta-analysis reveals consistency of allometric regressions, *Ecol. Model.*, 2007, **205**, 196–208.

30 D. W. van Valkengoed, E. H. J. Krekels and C. A. J. Knibbe, All You Need to Know About Allometric Scaling: An Integrative Review on the Theoretical Basis, Empirical Evidence, and Application in Human Pharmacology, *Clin. Pharmacokinet.*, 2025, **64**, 173–192.

31 C. D. Moyes and C. E. Genge, Scaling of muscle metabolic enzymes: An historical perspective, *Comp. Biochem. Physiol., Part A:Mol. Integr. Physiol.*, 2010, **156**, 344–350.

32 S. S. Killen, D. Atkinson and D. S. Glazier, The intraspecific scaling of metabolic rate with body mass in fishes depends on lifestyle and temperature, *Ecol. Lett.*, 2010, **13**, 184–193.

33 J. Raths, V. Švara, B. Lauper, Q. Fu and J. Hollender, Speed it up: How temperature drives toxicokinetics of organic contaminants in freshwater amphipods, *Glob. Change Biol.*, 2022.

34 Y. Liu, X. Luo, Y. Zeng, W. Tu, M. Deng, Y. Wu and B. Mai, Species-specific biomagnification and habitat-dependent trophic transfer of halogenated organic pollutants in insect-dominated food webs from an e-waste recycling site, *Environ. Int.*, 2020, **138**, 105674.

35 Y.-S. Lee, J. C. Lo, S. V. Otton, M. M. Moore, C. J. Kennedy and F. A. P. C. Gobas, In vitro to in vivo extrapolation of biotransformation rates for assessing bioaccumulation of hydrophobic organic chemicals in mammals, *Environ. Toxicol. Chem.*, 2017, **36**, 1934–1946.

36 C. J. Kennedy and K. B. Tierney, Energy intake affects the biotransformation rate, scope for induction, and metabolite profile of benzo[a]pyrene in rainbow trout, *Aquat. Toxicol.*, 2008, **90**, 172–181.

37 T. Sousa, T. Domingos, J. C. Poggiale and S. A. L. M. Kooijman, Dynamic energy budget theory restores coherence in biology, *Phil. Trans. Biol. Sci.*, 2010, **365**, 3413–3428.

38 S. A. L. M. Kooijman, *Dynamic Energy Budgets Theory for Metabolic Organisation*, Cambridge University Press, Cambridge, 2010.

39 J. A. Arnot and D. Mackay, Policies for Chemical Hazard and Risk Priority Setting: Can Persistence, Bioaccumulation, Toxicity, and Quantity Information Be Combined?, *Environ. Sci. Technol.*, 2008, **42**, 4648–4654.

40 S. B. Hedges, Amniote phylogeny and the position of turtles, *BMC Biol.*, 2012, **10**, 64.

41 R. B. B. d. Souza, V. M. G. Bonfim, V. P. Rios and W. Klein, Allometric relations of respiratory variables in Amniota: Effects of phylogeny, form, and function, *Comp. Biochem. Physiol., Part A:Mol. Integr. Physiol.*, 2021, **252**, 110845.

42 W. Dermauw, T. Van Leeuwen and R. Feyereisen, Diversity and evolution of the P450 family in arthropods, *Insect Biochem. Mol. Biol.*, 2020, **127**, 103490.

43 J. Haas, A. Hayward, B. Buer, F. Maiwald, B. Nebelsiek, J. Glaubitz, C. Bass and R. Nauen, Phylogenomic and functional characterization of an evolutionary conserved cytochrome P450-based insecticide detoxification mechanism in bees, *Proc. Natl. Acad. Sci. U. S. A.*, 2022, **119**, e2205850119.

44 J. Franklin, How reliable are field-derived biomagnification factors and trophic magnification factors as indicators of bioaccumulation potential? Conclusions from a case study on per- and polyfluoroalkyl substances, *Integrated Environ. Assess. Manag.*, 2016, **12**, 6–20.